

Soft Matter

Accepted Manuscript



This is an *Accepted Manuscript*, which has been through the Royal Society of Chemistry peer review process and has been accepted for publication.

Accepted Manuscripts are published online shortly after acceptance, before technical editing, formatting and proof reading. Using this free service, authors can make their results available to the community, in citable form, before we publish the edited article. We will replace this *Accepted Manuscript* with the edited and formatted *Advance Article* as soon as it is available.

You can find more information about *Accepted Manuscripts* in the [Information for Authors](#).

Please note that technical editing may introduce minor changes to the text and/or graphics, which may alter content. The journal's standard [Terms & Conditions](#) and the [Ethical guidelines](#) still apply. In no event shall the Royal Society of Chemistry be held responsible for any errors or omissions in this *Accepted Manuscript* or any consequences arising from the use of any information it contains.

ARTICLE

Anomalous long-range repulsion between silica surfaces induced by density inhomogeneities in supercritical ethanol

Cite this: DOI: 10.1039/x0xx00000x

Received 00th January 2012,
Accepted 00th January 2012

DOI: 10.1039/x0xx00000x

www.rsc.org/

Sada-atsu Mukai,^{a,b} Takehito Koyama,^{a,†} Kaoru Tsujii^c and Shigeru Deguchi^a

Anomalous long-range repulsion, extending over several micrometres, appears between silica surfaces at around the ridge of density fluctuations in supercritical ethanol at temperatures and pressures near the gas/liquid critical point ($T_c = 241$ °C, $P_c = 6.14$ MPa). Analysis shows that augmentation of ethanol density around silica surfaces in the presence of density fluctuations facilitates dissociation of silanol groups, leading to long-range electrostatic repulsion in the nonpolar medium.

Introduction

Supercritical fluids (SCFs) have attracted considerable interests as environmentally benign media for performing various chemical processes such as reactions, extraction, separation, and particle formation.¹ Density inhomogeneities distinguish SCFs from conventional solvents, as well as low viscosity and high diffusivity.² In the very close vicinity of the critical point, the compressibility diverges and correlation length of the density fluctuations becomes comparable to the wavelength of visible light, by which fluids scatter light strongly.³ The density fluctuations gradually diminish as the system goes away from the critical point, and form a ridge when the contour map of the intensities are projected on the phase diagram.^{4,5,6}

Large density inhomogeneities affect solvation of solute molecules in SCFs, because entropic penalty of bringing a solvent molecule to a high-density solvation layer is small and is easily compensated by enthalpic gain.^{2,7} For example, analysis of the fluorescent spectra of pyrene, which are sensitive indicators to the polarity of a surrounding local environment, in supercritical CO₂ (scCO₂) near the critical point showed that local solvent density around the pyrene molecules can be 1.5 – 1.7 times larger than the bulk density.⁸ Various chemical processes in SCFs, such as chemical reactions and energy transfer, are affected by the unique solvation.⁹

Koga et al. reported peculiar solvation of the surfaces of polymer films in scCO₂.¹⁰ Polymers such as styrene-butadiene copolymer, polystyrene, polybutadiene, and poly(methyl methacrylate) are not soluble in scCO₂, but the solvent quality of scCO₂ for the polymers dramatically change when the system was brought to temperature and pressures around the ridge, leading to abrupt and reversible swelling of the polymer

films. Interestingly, the swelling was surface specific and occurred only for the polymer chains in the close vicinity of the surface, whereas those in the bulk were not affected. The authors argued the surface-specific swelling of the polymers around the ridge was also ascribed to the increased compressibility of scCO₂ around the ridge.

Their results clearly demonstrate the anomalous solvation in SCFs occurs not only for small molecules, but also for macroscopic surfaces. However, our knowledge on the latter has been very sparse.¹¹ In this article, we show the density inhomogeneities in supercritical ethanol ($T_c = 241$ °C, $P_c = 6.14$ MPa, $\rho_c = 0.276$ g/cm³) induce anomalous solvation of silica surfaces and modulate local dielectric environments around the surfaces, leading to emergence of very long-range electrostatic repulsion between them.

Results

Long-range repulsion between silica surfaces in supercritical ethanol

We used an inverted optical microscope equipped with a high-temperature and high-pressure sample chamber,^{12,13} and examined structure of 2D arrays made of monodisperse silica particles ($d = 5.0$ μm) in supercritical ethanol.^{12,13} A dispersion of the silica particles in ethanol was introduced to the chamber, and the particles were allowed to sediment onto the surface of the bottom optical window made of diamond. As the window was tilted slightly (the tilt angle was estimated to be no larger than 0.6°), the particles were packed and formed an array near the periphery of the circular window due to gravity (Fig. S1). The entire system was then filled with ethanol, pressurised (typically to 36 MPa), and heated while maintaining the pressure. After the desired temperature was reached, pressure

was reduced isothermally (Fig. S2). Structural change of the arrays in the course of decompression was examined *in situ* from the bottom through the window.

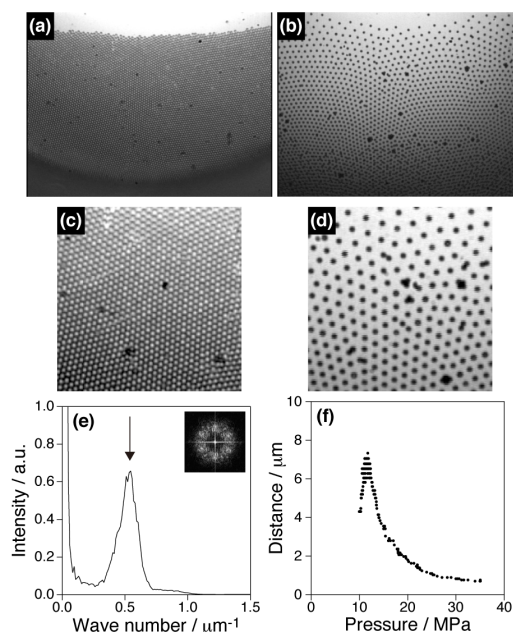


Fig. 1. Pressure-induced structural change of a 2D array of silica particles in supercritical ethanol. (a – d) *In situ* high-resolution optical microscopic images of a 2D array of monodisperse silica particles ($d = 5.0 \mu\text{m}$) formed on a diamond surface in supercritical ethanol at 306.8°C and at (a) 35.6 MPa and (b) 11.6 MPa . (c) and (d) represent magnified views of (a) and (b), respectively. (e) Radial distribution function calculated from (b). Inset shows a diffraction pattern. (f) Change of interparticle gap as a function of pressure at 306.8°C .

At 306.8°C and 35.6 MPa , the silica particles formed a hexagonal close-packed (hcp) array (Fig. 1a and 1c). The Brownian motion of the particles of this size was barely noticeable in ethanol at ambient temperature, but became evident in supercritical ethanol primarily due to a large decrease of the viscosity ($\eta_{(25^\circ\text{C}, 0.1 \text{ MPa})} = 1.085 \text{ mPa}\cdot\text{s}$, $\eta_{(306.8^\circ\text{C}, 35.6 \text{ MPa})} = 0.075 \text{ mPa}\cdot\text{s}$). When the pressure was decreased, however, the interparticle gap gradually increased while the particles retained a hexagonal arrangement (Fig. 1b, 1d and Movie S1).

To quantitatively analyse the structural change of the array, the microscopic image was Fourier-transformed to obtain a diffraction pattern (Fig. 1e, inset), from which a radial distribution function was calculated (Fig. 1e). An average minimum separation between the surfaces of adjacent particles was obtained by the position of the peak in the radial distribution function (indicated by an arrow in Fig. 1e), from which the diameter of the particle was subtracted to give the minimum separation between their surfaces (d_s) (Fig. 1f).

The d_s did not depend very much on the pressure between 36 and 25 MPa, but became highly pressure-dependent below $\sim 25 \text{ MPa}$. It increased continuously with the decrease of the pressure and reached $6.9 \mu\text{m}$ at 11.6 MPa . Further decrease of the pressure from 11.6 MPa led to steep contraction of d_s . The particles eventually adhered to the diamond surface and the Brownian motion completely ceased at 10 MPa (Movie S1).

The pressure-dependent structural change was reversible unless the pressure was decreased too low to induce the adhesion of the particles. The observation shows that anomalously long-range repulsive force, extending to $6.9 \mu\text{m}$, appeared between silica surfaces in supercritical ethanol at 11.6 MPa at 306.8°C .

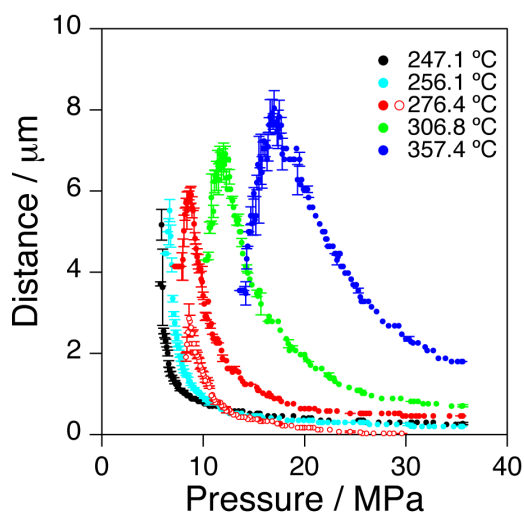


Fig. 2. Pressure dependent changes of d_s at different temperatures. Closed symbols denote experimental results obtained in pure ethanol. Open red circles represent results obtained in ethanol containing $1.9 \times 10^{-4} \text{ M}$ of NaNO_3 .

Similar pressure-dependent structural changes were observed in a wide temperature range between 247.1°C and 357.4°C (Fig. 2). At all temperatures, hcp arrays were formed at high pressures, and hexagonal non-contiguously close-packed (hnccp) arrays gradually appeared with the decrease of the pressure. The pressure dependence of d_s became less keen as the temperature was raised. Also, in each run, the pressure where largest d_s was observed shifted to higher pressures and largest d_s also increased with the temperature.

Effect of electrolyte and water

Pressure-dependent structural change was also observed when the experiment was performed in ethanol containing $1.9 \times 10^{-4} \text{ M}$ of NaNO_3 (open red circles in Fig. 2), but the observed d_s values were significantly smaller with the largest d_s of $2.9 \mu\text{m}$. Moreover, the d_s values decreased with the added NaNO_3 concentration, and the pressure-dependent structural change vanished in the presence of $\sim 1 \times 10^{-3} \text{ M}$ NaNO_3 (Fig. 3), indicating the long-range repulsion is of electrostatic origin.

At NaNO_3 concentrations higher than $2 \times 10^{-3} \text{ M}$, silica particles agglomerated and could no longer be dispersed individually (Fig. S3). The particles also adhered to the diamond surface and did not undergo Brownian motion at all. The result shows that silica particles were stabilised by short-range electrostatic repulsion even at high pressures and supports our previous observation on the dispersion stability of silica particles in supercritical ethanol.¹⁴ It also shows that there's electrostatic repulsion between the silica and diamond surfaces. Adhesion of the particles to the diamond surface at low pressure in supercritical ethanol without NaNO_3 (Movie

S1) would also be ascribed to loss of electrostatic repulsion between their surfaces. It is possible that properties of the diamond surface also changed depending on the temperature and pressure and affected the results. However, nothing has been known and possible such effect is not taken into account in the following discussion.

Deliberate addition of water to ethanol up to 5 wt%, on the other hand, did not affect the observed behaviour, indicating that effect of residual water in ethanol, such as preferential solvation, was not important in the emergence of the long-range repulsion.

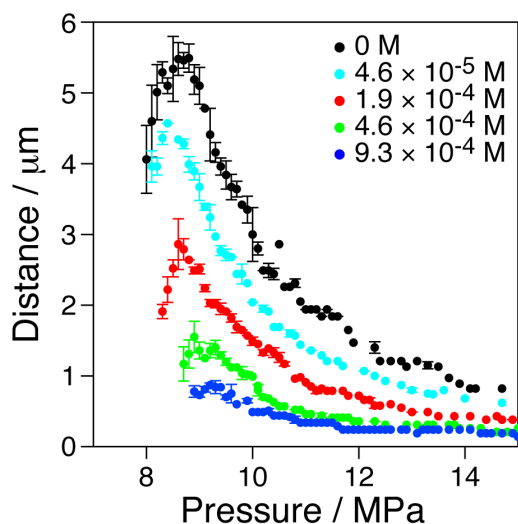


Fig. 3. Pressure dependent changes of d_s in supercritical ethanol containing various amount of NaNO_3 at 276.4 °C.

Density inhomogeneities of supercritical ethanol

Forces acting between surfaces play central roles in various colloidal phenomena such as self-assembly, adsorption/desorption, formulation, foam stability, and wetting.¹⁵ Electrostatic and van der Waals forces, the so-called Derjaguin-Landau-Verwey-Overbeek (DLVO) forces, are of primary importance, and the former is strongly affected by properties of the surface such as charge density.¹⁵ Our results show that extremely long-range electrostatic repulsion appeared between the silica surfaces in supercritical ethanol under certain sets of temperature and pressure.

The dielectric constant (ϵ) of supercritical ethanol is below 2 at temperatures and pressures where long-range repulsion was observed, the value of which is comparable to that of hydrocarbons (Fig. S4).¹⁶ On one hand, electrostatic repulsion between charged surfaces becomes long-ranged in such low- ϵ media.¹⁷ On the other hand, charging of silica surfaces through ionic dissociation of silanol groups is suppressed, which is the reason why silica particles do not disperse in low- ϵ media such as cyclohexane ($\epsilon = 2.0243$ at 20 °C).^{18,19} High thermal energy likely promotes dissociation of silanol groups, and this is a possible reason why the measured d_s values at 35 MPa, where pressure-dependent structural change almost vanished,

increased with temperature (Fig. 2). Nonetheless, our observation cannot be fully accounted for, because it indicates the surface charge density of silica particles increases specifically under certain sets of temperature and pressure, leading to long-range repulsion in a low- ϵ medium.

We found that there were pronounced density fluctuations under the conditions where long-range electrostatic repulsion was observed. From thermodynamic calculations, density fluctuation is described as

$$\frac{\langle(\Delta N)^2\rangle}{\langle N\rangle} = (N/V)\kappa_T k_B T \quad (1)$$

where N is the number of molecules in the volume V , k_B is the Boltzmann constant, κ_T is the isothermal compressibility, and T is the absolute temperature.⁵ By using density and isothermal compressibility that were calculated from the equation of state for ethanol (Figs. 4a and 4b), density fluctuations of supercritical ethanol under the present experimental conditions were calculated (Fig. 4c).

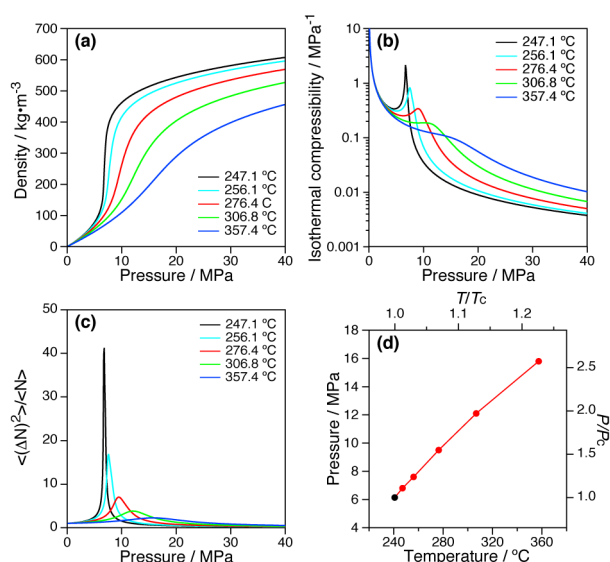


Fig. 4. Density fluctuations in supercritical ethanol. (a and b) Calculated density (a) and isothermal compressibility (b) of ethanol. (c) Density fluctuations in supercritical ethanol calculated according to eq. 1. (d) Sets of temperature and pressure where the density fluctuations become largest. Temperature and pressure that were normalised by critical temperature (T_c) and critical pressure (P_c) of ethanol, respectively, are also shown. Filled black symbol represents the gas/liquid critical point of ethanol.

Nishikawa et al. performed a series of scattering experiments, and showed that the density fluctuations form a sharp and intense peak near the critical point, but the peak broadened with temperature. Sets of temperature and pressure at which the density fluctuations peaked formed the “ridge” of density fluctuations extending from the critical point (Fig. 4d),⁵ which has also been known as Widom line.²⁰ The Widom line can be considered as extension of gas/liquid coexistence curve beyond the critical point. Experimental evidence has accumulated in the last decade showing that it indeed separates

supercritical fluids to a liquid-like and gas-like region, and various properties show sharp changes on crossing it.²¹

As can be seen in Figs. 5a-e, the pressure dependence of both d_s and density fluctuations showed good qualitative agreement, and the largest d_s was observed around the pressures where density fluctuations were most intense (Fig. 5f). These results suggest that the density fluctuations play an important role in the emergence of anomalous long-range electrostatic repulsion between silica surfaces in supercritical ethanol. The agreement was poor at low-pressure side of the peaks, especially at 357.4 °C, which may suggest that hydrodynamic interactions between silica surfaces and diamond surfaces become relevant at low pressures.¹³

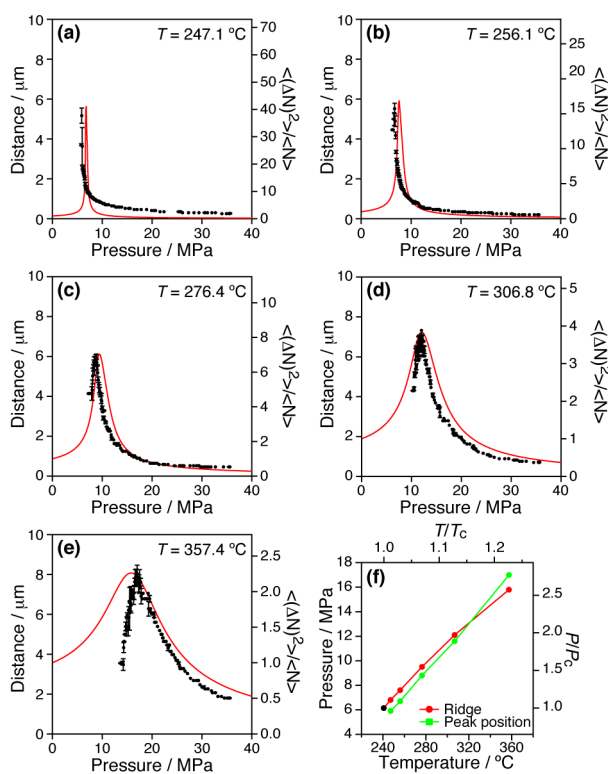


Fig. 5. (a-e) Comparison of the pressure dependence of d_s (black dots) and calculated density fluctuations (red curves). Vertical scales for the density fluctuations were normalised arbitrarily so that the peak heights of d_s and the density fluctuation became approximately the same. (f) Sets of temperature and pressure at which largest d_s was observed (green). The ridge of density fluctuations (Fig. 4d) is also shown (red).

Discussion

In considering surface charging of silica in heterogeneous media such as binary solvent mixtures, ϵ of local environment around the surface, not of the bulk, has to be considered.¹⁹ We propose the density augmentation of ethanol around the silica surface as a plausible mechanism behind the long-range electrostatic repulsion.

Like the density augmentation around small molecules in SCFs,² the density augmentation leads to larger local ϵ in the vicinity of silica surfaces, thereby promote surface charging by invoking dissociation of silanol groups. Such effect should

become most profound around the ridge of density fluctuations where density fluctuations are most pronounced, leading to anomalous long-range electrostatic repulsion in low- ϵ supercritical ethanol.

Mechanism for the density augmentation around small solutes can be divided into long-range inhomogeneities and local density inhomogeneities.² The extent of the former is governed by the correlation length of the density fluctuations, while the latter is governed by solvent-solute interactions.² Our results indicate the latter, interaction between the silica surface and ethanol, plays an important role in the emergence of the long-range repulsion.

An ethanol molecule has a permanent dipole moment and interact each other by hydrogen bonding. ¹H-NMR chemical shift measurements showed the hydrogen bonding between ethanol molecules persist even in the supercritical state, and the extent of hydrogen bonding at the present experimental conditions is estimated to be 20 to 40 % relative to ambient conditions.²² It is likely that the hydrogen bonding between ethanol and silica surfaces also persists in supercritical ethanol. The density fluctuations may facilitate structuring of ethanol on the silica surface via hydrogen bonding, such as those observed for silica surfaces in ethanol/cyclohexane mixtures.²³ Furthermore, a neighbouring group effect may come into play. A dissociated silanol group likely attracts more ethanol molecules and promotes further density augmentation, which in turn promotes dissociation of surrounding silanol groups on the silica surface.

Density inhomogeneity of various SCFs around the ridge of density fluctuations have been experimentally measured near the critical point up to $\sim 1.1 T/T_c$ or P/P_c .^{5, 6} In the case of supercritical ethanol, dynamic light scattering measurements showed the density fluctuations almost vanished at $1.06 T/T_c$.⁶ Accordingly, anomalies associated with density inhomogeneities in SCFs are typically observed in these temperature and pressure range.² A critical Casimir force,²⁴ which appears when the concentration fluctuations in a binary liquid mixture are confined between two surfaces, also appears only in the close vicinity of the critical point. In stark contrast, the long-range repulsion between the silica surfaces appeared even though the system was far from the critical point (up to $\sim 1.2 T/T_c$, $\sim 2.5 P/P_c$). Also, the largest d_s values observed at 247.1 °C ($1.01 T/T_c$) and 357.4 °C ($1.23 T/T_c$) were comparable despite a large difference in the intensity of the density fluctuation. No such results have been reported to the best of our knowledge. The results suggest that the long-range repulsion is very sensitive to the local density inhomogeneity around the silica surfaces. Presumably, even weak density fluctuation of the bulk would be sufficient to induce anomalous solvation and modulate the local dielectric environments around the silica surfaces.

Various charge-stabilised colloids coagulate rapidly in water when it is heated under pressure due to large decrease of ϵ .²⁵ In stark contrast, silica nanoparticles ($d = 60$ nm) remain stably dispersed even in low- ϵ supercritical ethanol, although numerical calculations using bulk properties of ethanol showed

the DLVO potential barrier between silica surfaces decrease to $2\text{--}5 k_B T$.¹⁴ The results would also be explained by taking into accounts specific interactions between silica surface and ethanol in supercritical ethanol.

Conclusions

We found that anomalous long-range electrostatic repulsion appeared between silica surfaces in supercritical ethanol around the ridge of density fluctuations. We propose that local density of ethanol around the silica surfaces is augmented, and facilitates ionic dissociation of surface silanol groups. Long-range electrostatic repulsion results due to low bulk dielectric constant of supercritical ethanol. Interaction between ethanol and silica surfaces likely plays a key role.

Experiments in other supercritical fluids are in progress to verify universality of our finding, which is one of the key basic properties of critical phenomena. The experiments would also help clarifying possible roles of solvent-surface interactions in the emergence of long-range electrostatic repulsion.

Experimental

Materials

Monodisperse silica particles (Hipresica, $d = 5.0 \mu\text{m}$) were obtained from Ube-Nitto Kasei Co., Ltd., Tokyo, Japan. Ethanol (>99.5% pure) and NaNO_3 were obtained from Wako Pure Chemical Industries, Ltd. (Osaka, Japan). Chemicals were used without further purification. Ethanol was kept in a desiccator to prevent the solvent from absorbing moisture in air. Properties (viscosity, density, and isothermal compressibility) of ethanol were calculated using the equation of state²⁶ on a NIST Reference Fluid Thermodynamic and Transport Properties Database (REFPROP) Version 8.0.18.

Preparation of 2D array

Silica particles were dispersed in ethanol at a concentration of approximately 0.3 mg/mL with the aid of ultrasonic agitation (Model 5510, 42 kHz output frequency, Branson Ultrasonic Corporation, Danbury, USA). The dispersion was loaded to a high-temperature and high-temperature sample chamber for optical microscopy. The chamber was made of titanium alloy and two optical windows made of diamond discs (1.5 mm diameter, 1 mm thick) were placed. The particles were then allowed to sediment on the surface of a bottom optical window. Once sedimentation was completed (took approximately 10 min), excess particles were removed by flushing the chamber with ethanol. Approximately $1 - 1.5 \times 10^4$ particles comprised the arrays examined in this study.

In situ microscopic observation

The chamber was connected to a pressurising system consisting of an HPLC pump (PU-2080, JASCO, Hachioji, Japan) and a back-pressure regulator (SCF-BPG/M, JASCO, Hachioji, Japan). The system was then pressurised by pumping ethanol,

and the specimen was heated while maintaining the high pressure. During heating, the particles were swept away to the periphery of the window due to convective flow. Once the sample reached a desired experimental temperature, pressure was controlled by a hand-operated high-pressure controller (AKICO, Tokyo, Japan). Temperature of the sample in the chamber was measured by a thermocouple that was calibrated by measuring the melting point of NaNO_3 (307 °C).¹⁸ Pressure of the system was measured by a sensor that was calibrated by using a Heise gauge (Model CMM dual pressure gauge, Ashcroft Inc., Stratford, USA). Structure of 2D array was observed by an inverted optical microscope (IX-71, Olympus, Tokyo, Japan), on which the sample chamber was set, with an optical resolution of $2 \mu\text{m}$.¹³

Acknowledgements

We thank Miki Yamamoto for stimulating discussions and Sayuki Ohta for technical assistance in the early stage of the work. This work was supported by Ground-Based Research Announcement for Space Utilization promoted by Japan Space Forum (to S.D., K.T. and S.M.), and Grant-in-Aid for young researchers (no 22740284 to T.K.) and for scientific research (no 22540495 to S.D. and T.K.) from the Japan Society for the Promotion of Science. S.M. acknowledges support by the Program for Improvement of Research Environment for Young Researchers from Special Coordination Funds for Promoting Science and Technology (SCF), Japan.

Notes and references

^a Research and Development Center for Marine Biosciences, Japan Agency for Marine-Earth Science and Technology (JAMSTEC), 2-15 Natsushima-cho, Yokosuka 237-0061, Japan. Fax: +81-46-867-9715; Tel: +81-46-867-9679; E-mail: shigeru.deguchi@jamstec.go.jp

^b Akiyoshi Bio-Nanotransporter Project, Exploratory Research for Advanced Technology (ERATO), Japan Science and Technology Agency (JST).

^c Research Institute for Electronic Science, Hokkaido University (retired).

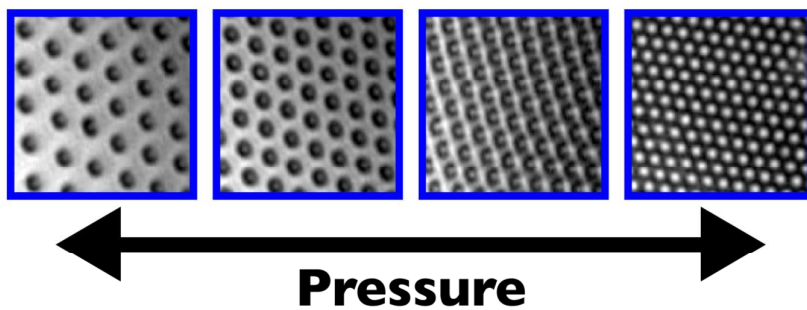
† Present address: Institute of Industrial Science, The University of Tokyo.

Electronic Supplementary Information (ESI) available: Figs. S1, S2, S3 and S4. Movie S1. See DOI: 10.1039/c000000x/

1. M. A. McHugh and V. J. Krukonsis, *Supercritical fluid extraction: principles and practice*, Butterworths, Boston, 1986; K. P. Johnston and J. M. Penninger, eds., *Supercritical Fluid Science and Technology*, American Chemical Society, Washington, DC, 1989.
2. S. C. Tucker, *Chem. Rev.*, 1999, **99**, 391–418.
3. H. E. Stanley, *Introduction to Phase Transition and Critical Phenomena*, Oxford University Press, Oxford, 1971.
4. T. Morita, K. Kusano, H. Ochiai, K. Saitow and K. Nishikawa, *J. Chem. Phys.*, 2000, **112**, 4203–4211; K. Nishikawa, K. Kusano, A. A. Arai and T. Morita, *J. Chem. Phys.*, 2003, **118**, 1341–1346; K. Saitow, D. Kajiya and K. Nishikawa, *J. Phys. Chem. A*, 2005, **109**, 83–91.

5. K. Nishikawa and T. Morita, *J. Supercrit. Fluids*, 1998, **13**, 143-148; K. Nishikawa, A. A. Arai and T. Morita, *J. Supercrit. Fluids*, 2004, **30**, 249-257.
6. D. Kajiya, K. Nishikawa and K. Saitow, *J. Phys. Chem. A*, 2005, **109**, 7365-7370.
7. S. C. Tucker and M. W. Maddox, *J. Phys. Chem. B*, 1998, **102**, 2437-2453.
8. J. Zhang, L. L. Lee and J. F. Brennecke, *J. Phys. Chem.*, 1995, **99**, 9268-9277.
9. O. Kajimoto, *Chem. Rev.*, 1999, **99**, 355-390.
10. T. Koga, Y.-S. Seo, Y. Zhang, K. Shin, K. Kusano, K. Nishikawa, M. H. Rafailovich, J. C. Sokolov, B. Chu, D. Peiffer, R. Occhiogrosso and S. K. Satija, *Phys. Rev. Lett.*, 2002, **89**, 125506; T. Koga, Y.-S. Seo, K. Shin, Y. Zhang, M. H. Rafailovich, J. C. Sokolov, B. Chu and S. K. Satija, *Macromolecules*, 2003, **36**, 5236-5243.
11. S. Deguchi and K. Tsujii, *Soft Matter*, 2007, **3**, 797-803.
12. S. Deguchi and K. Tsujii, *Rev. Sci. Instrum.*, 2002, **73**, 3938-3941.
13. S. Mukai, S. Deguchi and K. Tsujii, *Colloids Surf., A*, 2006, **282-283**, 483-488.
14. S. K. Ghosh, S. Mukai, S. Deguchi and K. Tsujii, *J. Phys. Chem. B*, 2007, **111**, 8169-8174.
15. J. Israelachvili, *Intermolecular and Surface Forces*, Academic Press, London, 1992; D. F. Evans and H. Wennerström, *The Colloidal Domain*, 2nd edn., Wiley-VCH, New York, 1999.
16. Y. Hiejima and M. Yao, *J. Chem. Phys.*, 2003, **119**, 7931-7942.
17. J. Lyklema, *Adv. Colloid Interface Sci.*, 1968, **2**, 65-114.
18. D. R. Lide, ed., *CRC Handbook of Chemistry and Physics*, 76th edn., CRC Press, Boca Raton, 1994.
19. B. Vincent, Z. Király, S. Emmett and A. Beaver, *Colloids Surf.*, 1990, **49**, 121-132.
20. B. Widom, in *Phase Transition and Critical Phenomena*, eds. C. Domb and M. S. Green, Academic Press, London, 1972, vol. 2.
21. L. M. Xu, P. Kumar, S. V. Buldyrev, S. H. Chen, P. H. Poole, F. Sciortino and H. E. Stanley, *Proc. Natl. Acad. Sci. U.S.A.*, 2005, **102**, 16558-16562; G. G. Simeoni, T. Bryk, F. A. Gorelli, M. Krisch, G. Ruocco, M. Santoro and T. Scopigno, *Nature Phys.*, 2010, **6**, 503-507; A. R. Imre, U. K. Deiters, T. Kraska and I. Tiselj, *Nucl. Eng. Des.*, 2012, **252**, 179-183.
22. M. M. Hoffmann and M. S. Conradi, *J. Phys. Chem. B*, 1998, **102**, 263-271.
23. M. Mizukami, M. Moteki and K. Kurihara, *J. Am. Chem. Soc.*, 2002, **124**, 12889-12897.
24. C. Hertlein, L. Helden, A. Gambassi, S. Dietrich and C. Bechinger, *Nature*, 2008, **451**, 172-175.
25. R. G. Alargova, S. Deguchi and K. Tsujii, *Colloids Surf., A*, 2001, **183-185**, 303-312; S. K. Ghosh, R. G. Alargova, S. Deguchi and K. Tsujii, *J. Phys. Chem. B*, 2006, **110**, 25901-25907; R. G. Alargova and K. Tsujii, *Prog. Colloid Polym. Sci.*, 2004, **126**, 134-138.
26. H. E. Dillon and S. G. Penoncello, *Int. J. Thermophys.*, 2004, **25**, 321-335.

Graphical and textual abstract for “Anomalous long-range repulsion between silica surfaces induced by density inhomogeneities in supercritical ethanol” by S. Mukai, T. Koyama, K. Tsujii and S. Deguchi



Long-range repulsion, extending over several μm , emerged between silica surfaces around the ridge of the density fluctuations in supercritical ethanol.